Efficient measurement of an optical orbital-angular-momentum spectrum comprising more than 50 states

2013 New J. Phys. 15 013024

(http://iopscience.iop.org/1367-2630/15/1/013024)

New Journal of Physics
The open access journal for physics

Efficient measurement of an optical orbital-angular-momentum spectrum comprising more than 50 states

Martin P J Lavery[1,6], David J Robertson[2], Anna Sponselli[3], Johannes Courtial[1], Nicholas K Steinhoff[4], Glenn A Tyler[4], Alan E Willner[5] and Miles J Padgett[1]

[1] School of Physics and Astronomy, University of Glasgow, Glasgow, UK
[2] Centre for Advanced Instrumentation, Department of Physics, Durham University, Durham DH1 3LE, UK
[3] Department of Physics and Astronomy, University of Padova, Vicolo dell'Osservatorio 3, I-35122 Padova, Italy
[4] The Optical Sciences Company, 1341 S Sunkist Street, Anaheim, CA 92806-5614, USA
[5] Department of Electrical Engineering, University of Southern California, Los Angeles, CA 90089, USA
E-mail: m.lavery@physics.gla.ac.uk

New Journal of Physics **15** (2013) 013024 (7pp)
Received 10 September 2012
Published 14 January 2013
Online at http://www.njp.org/
doi:10.1088/1367-2630/15/1/013024

Abstract. A light beam may be separated into its orbital-angular momentum (OAM) components by a geometric optical transformation that converts each OAM component into a plane wave with a transverse phase gradient. Subsequent focusing produces a spot the lateral position of which is proportional to the input OAM state (Lavery *et al* 2012 *Opt. Express* **20** 3). In this paper, we improve this approach, extending the measurement bandwidth to >50 OAM states and showing a simultaneous measurement of the radial coordinate.

[6] Author to whom any correspondence should be addressed.

The necessity to transmit ever larger amounts of data across networks constantly pushes the information bandwidth of optical communication systems. In an attempt to increase the available bandwidth, the use of optical characteristics other than polarization, wavelength and intensity is of interest to many researchers in the optical communication field. One such additional characteristic is orbital-angular momentum (OAM) [1]. Allen *et al* showed that beams with a transverse complex amplitude profile of the form $\psi_\ell = A(r)\exp(\mathrm{i}\ell\theta)$, where r and θ are the radial and azimuthal coordinates, respectively, and $A(r)$ is the radial amplitude, carry an OAM of $\ell\hbar$ per photon [1–3]. The variable ℓ is an integer that is, in principle, unbounded, potentially leading to a larger alphabet for optical communications [4–9]. In addition to classical considerations, this larger alphabet has been suggested as a way of improving the security of cryptographic keys transmitted with a quantum-key-distribution system [10–12].

We recently developed an optical device (mode sorter (MS)) comprising two free-form refractive optical elements that can be used to transform OAM states into transverse momentum states [13, 14]. Acting together, these elements map a polar position (r, θ) in the input plane to a corresponding Cartesian position (x, y) in the output plane such that $x = \ln(r)$ and $y = \theta$, while preserving the relative phase of adjacent points within the beam [13]. This MS transforms a set of concentric rings at the input plane into a set of parallel lines in the output plane [15, 16] and, as it preserves relative phase, it therefore transforms an azimuthal phase gradient into a transverse phase gradient, i.e. OAM states into transverse momentum states. A spherical lens placed behind the second element then focuses the resulting transverse momentum states into specified lateral positions with Cartesian coordinates (u, v) in its back focal plane. Detectors in those positions can therefore measure the power in different superpositions of OAM states—the OAM spectrum—of light incident on the MS [17, 18].

Key to reliable position mapping is that the transformed coordinates x and y should depend only on the coordinates r and θ that determine the position in the input plane of a light ray, and not on the ray's direction. Our MS works by the first element introducing a spatially dependent deviation to the ray direction, such that upon propagation to the second element the ray arrives at the required position with the Cartesian coordinates x and y. The role of the second element is to ensure that relative phase is preserved. The elements are designed to work perfectly for collimated beams, in which all light rays arrive at normal incidence at the first component. For non-collimated beams we require that the angular deviation introduced by the reformatter dominates over any deviation from normal incidence with which rays arrive at the first element. If the input OAM beam is an annulus of radius r and the separation between the two elements is L, then the angular deviation introduced by the sorter is of the order of $\tan^{-1}(r/L)$, which is approximately r/L for small angles. Deviations from normal incidence of ray directions in the incident beam can be due to beam divergence, alignment or other properties. Irrespective of their divergence, beams carrying OAM are never plane waves as it is an azimuthal component to the Poynting vector that gives such beams their angular momentum in the direction of propagation (figure 1). For a beam described by an azimuthal phase term $\exp(\mathrm{i}\ell\theta)$, the local skew angle of the Poynting vector in the azimuthal direction is given by $\tan^{-1}(\ell/kr)$ [19, 20]. Close to the beam axis, i.e. for $r \approx 0$, this skew angle reaches 90°, and so the deviation introduced by the sorter cannot dominate, but conveniently OAM states with $\ell \neq 0$ are dark along their axis. It follows that for the sorter to work well for beams of radius r, we require $\ell/kr \ll r/L$, which gives (with $k = 2\pi/\lambda$)

$$\ell \ll \frac{2\pi r^2}{L\lambda}. \tag{1}$$

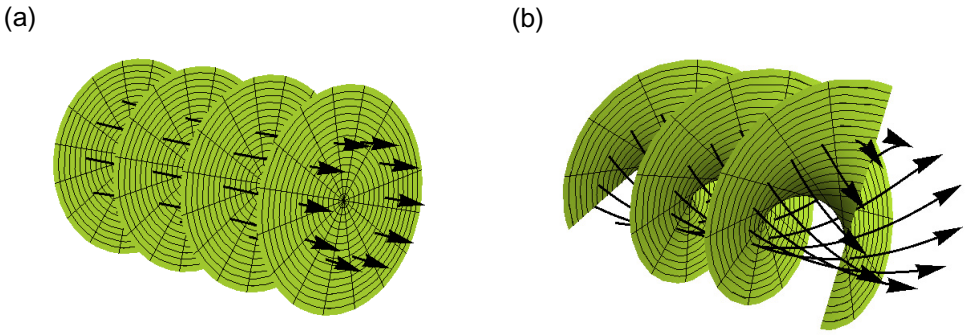

Figure 1. The local ray direction, shown as arrows, is perpendicular to the phase fronts, shown as green surfaces. (a) In beams with $\ell = 0$, the local ray direction has no azimuthal component. (b) In beams with $\ell \neq 0$, the local ray direction does have an azimuthal component. The figure is drawn for $\ell = 2$.

We note that the rhs of this equation reaches its maximum value when the radius of the input beam matches the radius of the optical element and then the rhs is essentially the Fresnel number of the optical elements. The main result of this paper is the demonstration of an optical mapper comprising components whose Fresnel number is sufficient to distinguish more than 50 OAM states.

In addition to increasing the measurement bandwidth, we present a further modification which allows measurement of the full radius-OAM spectrum, i.e. the OAM spectrum present at different radii r in the incident beam, simultaneously for all values of r. The MS maps any centred, thin ring of light of radius, r, to a thin line with a corresponding x-coordinate. However, the OAM spectrum cannot be deduced, as this requires Fourier transformation. A subsequent spherical Fourier lens performs this Fourier transform and therefore allows measurement of the OAM spectrum, but loses all information about r. Our solution is to combine the spherical Fourier lens with a cylindrical lens. This combination can be thought of as two orthogonal cylindrical lenses of different focal lengths, one performing an optical Fourier transform of the y-coordinate and the other imaging the x-coordinate. It is then possible to measure the OAM spectrum simultaneously for all values of the radial coordinate.

To maximize the Fresnel number and therefore OAM bandwidth, we designed our free-form optical elements such that they have the largest aperture that can be achieved by our method of manufacture ($R = 12$ mm) and the shortest possible separation between the optical elements ($L = 300$ mm), which is limited by the maximum surface gradient that can be machined. The resulting Fresnel number is $F = R^2/L\lambda \approx 760$. However, for measuring laser beams of finite size, we note that the effective Fresnel number of the system is set by the radius of the optics, or the radius of the beam itself, whichever is smaller. The elements were diamond machined using a Nanotech three-axis ultra-precision lathe in combination with a Nanotech NFTS6000 fast tool servo system to provide a fast axis superimposed on one of the axes of the lathe. The increase in the aperture size results in deeper cuts as the overall thickness variation of the surface has increased. A vacuum chuck is generally used in such a lathe; however, due to the large cut depth a semi-permanent bonding technique is used. A water-soluble wax, produced by Nexgen Optical, was used as the bonding agent as this can easily be de-bonded with the use of a standard ultrasonic system. The output plane of the MS was focused to the plane of the detector using a

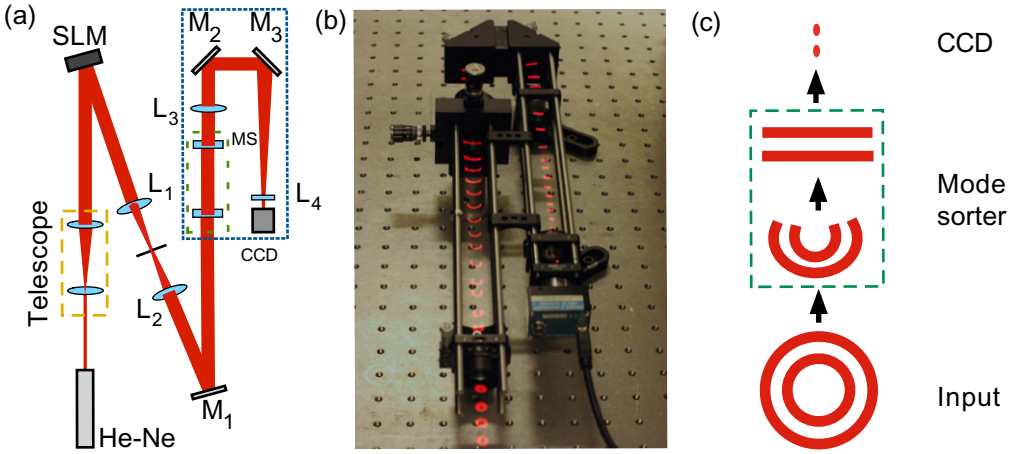

Figure 2. (a) A beam carrying OAM is prepared through the use of an ℓ-forked hologram, realized using a spatial light modulator (SLM), and a Fourier filter (lenses L_1 and L_2 and the aperture between them) that selects the desired first diffraction order. The beam is then passed through the optical reformatter, i.e. the two custom refractive components in the green dashed box. The spherical lens L_3 and the cylindrical lens L_4 complete the transformation of the beam. Together, the components in the blue dashed box form the MS. (b) Photograph of the MS realized in the laboratory. An image of the beam was captured in several transverse planes and overlaid (in red), showing the shape of the beam in those planes. (c) Schematic diagram of the beam transformation performed by the MS.

spherical lens (L_3 in figure 2; focal length $f_3 = 500\,\text{mm}$) in combination with a cylindrical lens (L_4; focal length $f_4 = 40\,\text{mm}$), giving a lateral displacement of 17.6 μm for an increase $\Delta\ell = 1$ in OAM value and a radial magnification of 0.096.

We generate the input OAM test modes by the use of a simple forked diffraction grating created using an SLM that is illuminated by the expanded Gaussian beam produced by a HeNe laser [21, 22]. This results in a helically phased beam with a Gaussian intensity distribution. To obtain radial control of the intensity distribution we apply a spatially dependent reduction of the contrast, allowing us to create in the first-order diffracted beam a close approximation of any Laguerre–Gaussian mode of choice [23]. This approach allows control over the beam waist w_0 independent of the mode index. The SLM is then imaged to the input pupil of the OAM MS. Varying w_0 therefore allows measurement of the OAM bandwidth for different effective Fresnel numbers.

We generate a set of sequential input modes over the range $\ell = -28$ to +28 with a specific w_0. Three different values of w_0 were tested for the same set of ℓ-values, corresponding to three different effective Fresnel numbers. A CCD array was placed at the focal plane of the final lens where adjacent, equally sized regions were defined, each corresponding to a specific ℓ-value. The total intensity over all the pixels in each region was summed to give the relative power in each of the OAM modes. As discussed in our earlier work, this approach has some residual crosstalk that can be deduced by considering the focal spot produced from a top-hat aperture [13, 14]. In our case, the transformation of a set of concentric rings of light at the input to parallel lines, with finite extent, at the output results in a Sinc distribution when such an

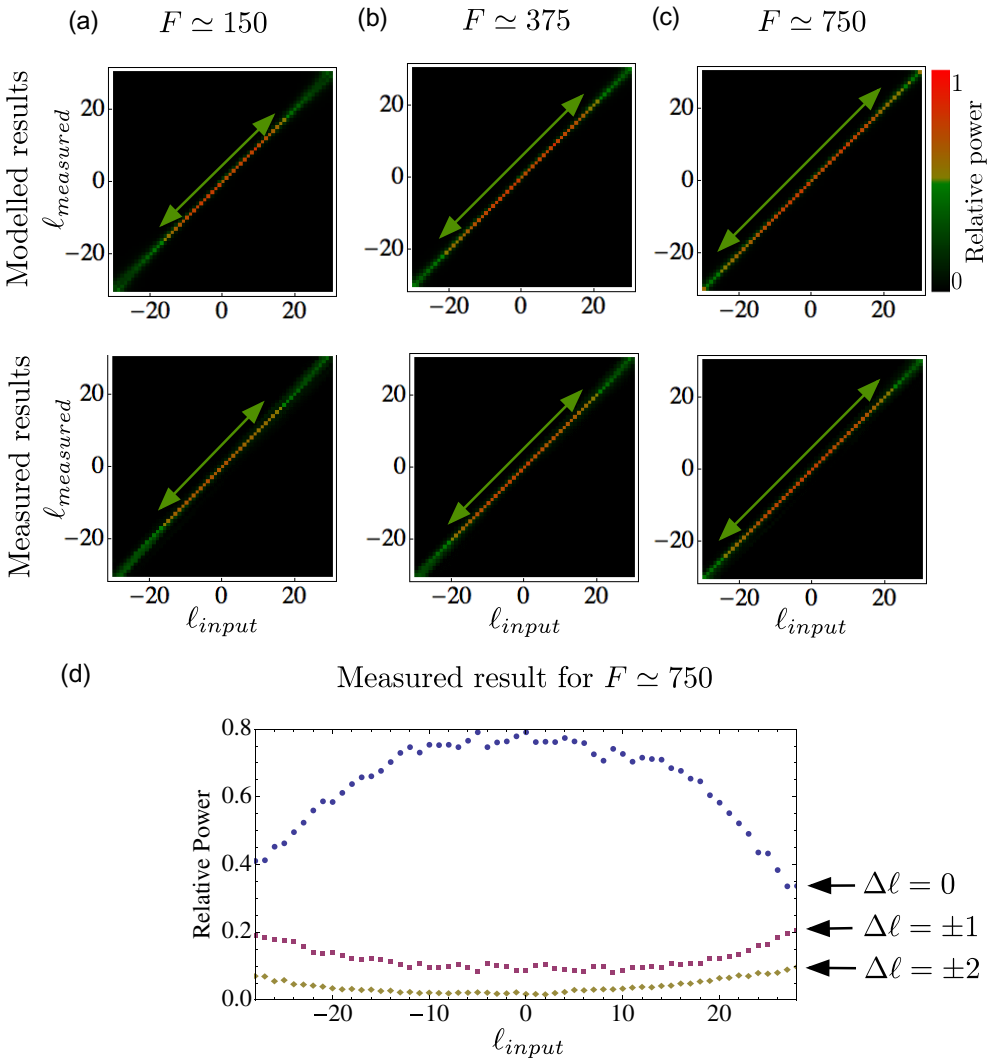

Figure 3. (a)–(c) Colour representation of the power in the bins corresponding to OAM states with $\ell = \ell_{\text{measured}}$ for incident pure OAM modes with $\ell = \ell_{\text{input}}$. The columns (a)–(c) correspond to different effective Fresnel numbers of the system, which was achieved by changing the waist size w_0 of the input mode. In each column, modelled (top) and measured (bottom) results are shown. The green arrows indicate the measurement bandwidth where the measured relative power is greater than 0.5. (d) Fraction of power in the bins corresponding to $\Delta\ell = \ell_{\text{input}} - \ell_{\text{measured}}$. The top set of points (in blue) represents power that has been correctly identified; here $\ell_{\text{input}} = \ell_{\text{measured}}$ giving $\Delta\ell = 0$. The two lower sets of points are the sum of the power in the bins $\Delta\ell = \pm 1$ (in pink), where $\ell_{\text{measured}} = \ell_{\text{input}} + 1$ and $\ell_{\text{measured}} = \ell_{\text{input}} - 1$, and $\Delta\ell = \pm 2$ (in brown) which both represent crosstalk.

output is focused. The secondary maxima of the Sinc distribution give crosstalk into adjacent OAM channels. This predicts that, for low ℓ-values, approximately 80% of the input light will be present in the correct bin [14]. Our results (figure 3(a)) show an increase in crosstalk for higher

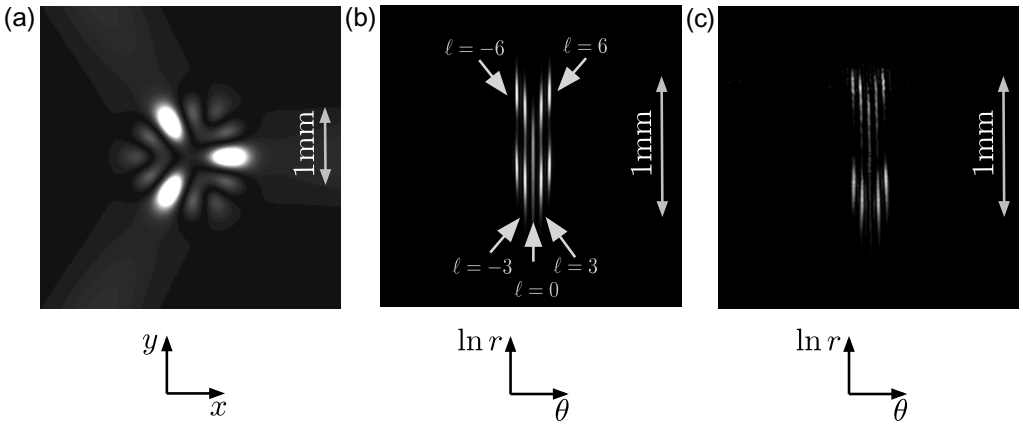

Figure 4. Simulated and measured radius-OAM spectra of a light beam. (a) Simulated intensity cross-section of the incident light beam, a superposition of Laguerre–Gauss modes with $\ell = -6, -3, 0, 3, 6$ and waist size $w_0 = 2\,\text{mm}$ and with $\ell = -6, -3, 3, 6$ and waist size $w_0 = 0.4\,\text{mm}$. The contrast has been altered to increase the visibility of the darker parts of the beam. (b), (c) Simulated (b) and measured (c) radius-OAM spectra of the beam.

ℓ-values in the form of a blurring of the diagonal, which is consistent with the higher skew angles present in such beams. When the effective Fresnel number is increased, this crosstalk at higher ℓ-values is reduced (figures 3(b) and (c)). All our experimental results are in close agreement with a model based upon plane-wave decomposition.

To show that our setup can measure OAM and r simultaneously, we generated a superposition of nine different modes. Both numerically modelled and experimentally measured radius-OAM outputs as measured by the CCD array are shown in figure 4. It should be noted that sorting of different beam waist can increase the available channels, but as the effective Fresnel number of the system is different for each value of w_0, smaller beams have a more restricted ℓ bandwidth.

In conclusion, we have presented a scalable solution to increasing the available OAM bandwidth of an MS based on optical reformatting, and we have demonstrated that this works by measuring OAM spectra of over 50 ℓ-values. We have also modified the setup so that the OAM spectrum can be measured as a function of r. We believe that these improvements will increase the feasibility of such a measurement technique being implemented as a tool in the fields of optical communication and quantum optics.

Acknowledgments

The authors acknowledge Daniel J Gauthier for useful discussions. This research was supported by the EPSRC and the DARPA InPho programme through the US Army Research Office award W911NF-10-1-0395. Our work was carried out as part of the European collaboration EC FP7 255914, PHORBITECH. MJP is supported by the Royal Society.

References

[1] Allen L *et al* 1992 *Phys. Rev.* A **45** 8185
[2] Yao A M and Padgett M J 2011 *Adv. Opt. Photon.* **3** 161
[3] Molina-Terriza G, Torres J P and Torner L 2001 *Phys. Rev. Lett.* **88** 013601
[4] Gibson G *et al* 2004 *Opt. Express* **12** 5448
[5] Leach J *et al* 2010 *Science* **329** 662
[6] Tamburiniand F *et al* 2012 *New J. Phys.* **14** 033001
[7] Wang J *et al* 2012 *Nature Photon.* **6** 488
[8] Bozinovic N *et al* 2012 *Opt. Lett.* **37** 2451–3
[9] Yan Y 2012 *Opt. Lett.* **37** 17
[10] Bourennane M, Karlsson A and Björk G 2001 *Phys. Rev.* A **64** 012306
[11] Malik M *et al* 2012 *Opt. Express* **20** 1319513200
[12] Vaziri A, Weihs G and Zeilinger A 2002 *Phys. Rev. Lett.* **89** 240401
[13] Berkhout G C G *et al* 2010 *Phys. Rev. Lett.* **105** 153601
[14] Lavery M *et al* 2012 *Opt. Express* **20** 3
[15] Bryngdahl O 1974 *J. Opt. Soc. Am.* **64** 1092–9
[16] Hossack W, Darling A and Dahdour A 1987 *J. Mod. Opt.* **34** 1235–50
[17] Lavery M P J, Berkhout G C G, Courtial J and Padgett M J 2011 *J. Opt.* **13** 064006
[18] Berkhout G C G, Lavery M P J, Beijersbergen M W and Padgett M J 2011 *Opt. Lett.* **36** 1863–5
[19] Padgett M J and Allen L 1995 *Opt. Commun.* **121** 36
[20] Berry M V and McDonald K T 2008 *J. Opt. A: Pure Appl. Opt.* **10** 035005
[21] Bazhenov V, Soskin M and Vasnetsov M 1992 *J. Mod. Opt.* **39** 985–90
[22] Heckenberg N, McDuff R, Smith C and White A 1992 *Opt. Lett.* **17** 221–3
[23] Leach J *et al* 2005 *New J. Phys.* **7** 55